Progress In Electromagnetics Research C, Vol. 114, 13–29, 2021

Multiple-Input Multiple-Output Antenna for Sub-Six GHz 5G Applications Using Coupled Folded Antenna with Defective Ground Surface

Alaa M. Hediya[1], Ahmed M. Attiya[2], and Walid S. El-Deeb[3, *]

Abstract—A 6-element MIMO antenna system is introduced in this paper for N77, N78, and N79 (5G) communication bands. The proposed antenna element is composed of a four-section coupled line folded antenna. The performance of this antenna element is improved by using a partial ground plane combined with the DGS between the different elements of the MIMO antenna. The separated single antenna in this case has a reflection coefficient less than −10 dB over the frequency band from 3 GHz to 5 GHz. For the complete MIMO configuration, the reflection coefficient is less than −7 dB over the same frequency band for all the antenna elements. On the other hand, the isolation between antenna elements in the MIMO configuration is greater than 15 dB. The values of the MIMO parameters are calculated. These parameters include the Envelope Correlation Coefficient between the different elements (ECC), Diversity gain (DG), Total Active Reflection Coefficient (TARC), Channel Capacity Loss (CCL), and Mean Effective Gain (MEG). Good results are obtained for the MIMO parameters where $ECC < 0.006$, $DG = 10$, $TARC < -7$, $CLL < 0.6$, and $-3 < MEG < -8$. These performance parameters of the proposed MIMO system indicate that this antenna is suitable for 5G applications. The effect of the human hand on the S-parameter is also investigated. The proposed antenna is fabricated and measured to verify the simulation results.

1. INTRODUCTION

In the past decades, the field of mobile communication has evolved greatly, due to the increasing demands of wireless traffic. This had a great impact on economic and social development and also led to the emergence of the fifth-generation (5G) technology as a fundamental basis for the future generation. The most commonly used 5G New Radio (NR) system bands are three main bands: N77 (3.3–4.2 GHz), N78 (3.3–3.8 GHz), and N79 (4.4–5.0 GHz) [1–3].

The key technique used to reach the requirements of 5G communications, which is to enhance channel capacity and improve communication performance without providing additional bandwidth (BW), is the Multiple-Input-Multiple-Output (MIMO) wireless system technique. MIMO system technique is characterized by the presence of multiple antenna elements in the transmitter and in the receiver. This is suitable to improve the system performance without increasing power at the source. That is because MIMO systems can transmit multiple signals simultaneously with average power levels [4].

There are considerable challenges that face the design of the MIMO system. The first challenge is producing an antenna of compact size. The second challenge is achieving acceptable isolations between the radiating elements. A trade-off is made between achieving the required isolation values and achieving

Received 3 May 2021, Accepted 1 July 2021, Scheduled 11 July 2021

* Corresponding author: Walid S. El-Deeb (wseldeeb@ucalgary.ca).

[1] Electronics and Communications Engineering Department, Zagazig Higher Institute of Engineering and Technology, Zagazig, Egypt. [2] Microwave Engineering Department, Electronics Research Institute (ERI), Cairo, Egypt. [3] Electronics and Communications Engineering Department, Faculty of Engineering, Zagazig University, Zagazig, Egypt.

the acceptable performance of the antenna. That is because when the isolation decreases, the mutual coupling that occurs between adjacent antennas increases. Thus, the overall system's performance in terms of gain and directivity is improved [5].

To face the first challenge, it is required to use an antenna that gives high efficiency and wide bandwidth with a small size. This can be performed by employing the modified folded dipole antenna that commonly used in the fifth generation of mobile phones instead of using the traditional type of folded dipole antenna which supports low and narrow bandwidth. Hu et al. modified a compact size folded dipole antenna to achieve 80% broad bandwidth and antenna gain around 1.27 dBi [6].

To overcome the second challenge, several decoupling methods have been developed to achieve an acceptable level of isolation between antennas while increasing the impedance bandwidth and improve the antenna matching as well. This can be performed by inserting a Frequency Selective Surface (FSS) structure or inserting an Electromagnetic Band Gap (EBG) structure. Banerjee et al. used a defective ground plane structure with a MIMO system to obtain ultra-wideband and high isolation from 14.71 to 21.81 dB [7]. Rao et al. designed a MIMO antenna system with a defective ground structure and achieved ultra-wideband with good isolation [8]. When a defective ground structure is designed, one of the most important parameters that must be taken into account is the return loss, because with changing the dimensions of the Defective Ground Surface (DGS) the resonant frequency changes as well. Hota et al. designed a modified circular patch planner antenna with a DGS and achieved an efficiency of 73.5% and an antenna gain of 3.5 dBi [9].

The use of a DGS is suitable to reduce the antenna area interacting with the human body. Thus, the technique may also contribute to reducing the specific absorption coefficient (SAR), while maintaining the impedance bandwidth of the antenna [10]. Bhattacharjee et al. designed an antenna with a defective ground structure to reduce the SAR value by 25.5% with an impedance bandwidth of 69.04% [11]. When designing the DGS, one of the most important parameters that must be taken into account is the return loss because with changing the dimensions of the DGS the resonant frequency changes. Thus, DGS can be used to improve the antenna matching too. Hota et al. designed a modified circular patch planner antenna with a DGS and achieved an efficiency of 73.5%, and an antenna gain of 3.5 dBi [12].

The choice of the material for the substrate is another important issue in the design of the proposed antenna. FR-4 represents a quite popular material that is suitable for different electrical and mechanical applications. Among the features of FR-4 material, which make it suitable for use in mobile applications, are high mechanical values, electrical insulating qualities, good fabrication characteristics, and low permittivity. These features made it easy to manufacture, safe to use, good in insulation, and suitable for wideband applications. It can also achieve high efficiency and small size [13, 14].

In this paper, a new modification for a traditional folded dipole antenna is presented. The modified design operates in the sub-six GHz 5G bands, N77, N78, and N79 simultaneously, with a bandwidth from 3 GHz to 5 GHz. The proposed coupled-folded antenna is created by dividing the traditional folded dipole antenna into four coupled sections on an FR-4 substrate. Additionally, a partial ground plane is used to achieve wide bandwidth. The spacing between the coupled-folded antennas is covered by DGS to improve the performance of the single element and the overall performance of the MIMO configuration. With this arrangement, the first and second resonance modes of the conventional folded dipole antenna at 0.5λ and 1.0λ, respectively, still exist. Besides, a new resonance mode at 0.25λ can be excited. The combination of the three modes, 0.25λ, 0.5λ, and 1.0λ, forms a very wide bandwidth that covers the whole frequency range of (3.0–5.0) GHz. A wide bandwidth 6-antennas MIMO system is also investigated. The DGS was also used to improve the isolation between the MIMO antenna elements. The proposed coupled-loop antenna and the MIMO system are simulated using CST Microwave Studio, and also fabricated and measured for the verification of the obtained results.

2. ANTENNA ELEMENT

The geometry of the proposed coupled folded antenna structure with dimension details in millimeters is shown in Figure 1. It consists of four L-shape capacitively coupled sections. The operating bandwidth and efficiency of this structure can be adjusted by adjusting the spacing between L-shape sections and the lengths of the coupled parts between them. The proposed antenna is printed on a 0.8 mm thick FR-4 substrate with a permittivity (ε_r) of 4.3 and loss tangent of 0.01. The overall dimension of the

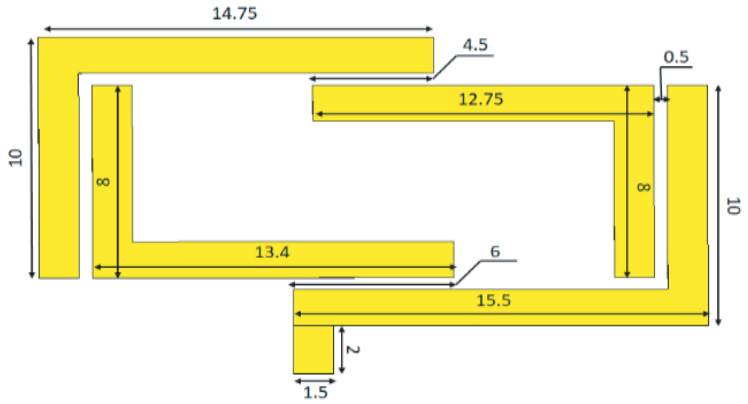

Figure 1. The detailed geometry of the proposed antenna folded dipole (all dimensions in mm).

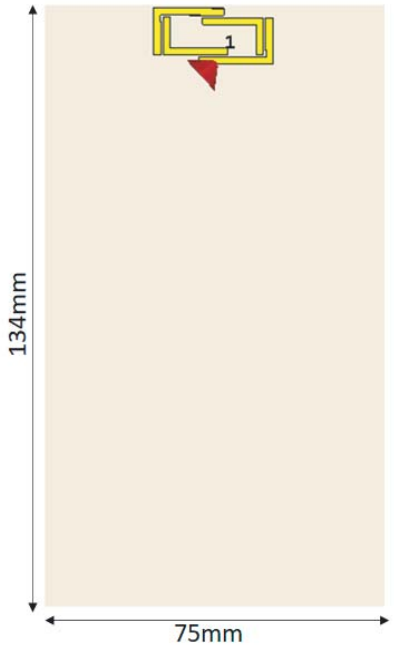

Figure 2. The Complete geometry of the folded dipole on a substrate of a size of a mobile phone.

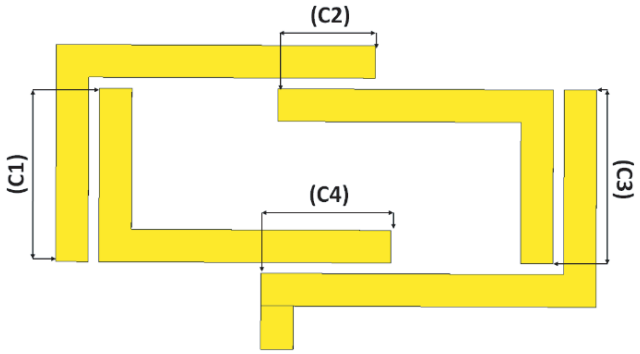

Figure 3. The capacitors are produced due to coupled sections.

individual antenna is $25 \times 12 \times 0.8\,\text{mm}^3$. The antenna is designed on a mobile phone board with an overall dimension of $75 \times 134 \times 0.8\,\text{mm}^3$ as shown in Figure 2.

Traditionally, the first and second modes of a folded dipole antenna are at effective lengths (0.5λ) and (1.0λ), respectively. However, the length of the proposed four sections of coupled folded antenna is less than the value of 0.5λ and roughly equal to 0.25λ. This is due to the effect of the coupled sections where each section produces a capacitance whose value varies according to the length of the coupled section, the space between coupled sections, and the thickness of these sections. This capacitance controls the total input impedance of the antenna and therefore controls the length of the antenna that achieves the resonance. Figure 3, shows how to adjust the various capacitances along with the proposed folded antenna. It can be noted that the total length of the antenna is affected by capacitances C2 and C4, while the width of the antenna is affected by capacitances C1 and C3. Ultimately, they all affect

the resonant frequency of the antenna element.

Three different cases are studied for this antenna configuration. In the first case, the antenna is designed with a full ground plane on the backside of the substrate. In the second case, a partial ground plane was used to increase the BW and also because it has a great role in improving the efficiency of the antenna [15]. The partial ground plane is used as shown in Figure 4(a), where the ground plane is removed only from the space behind the proposed coupled loop antenna, where $Lg = 14\,\text{mm}$. In the third case, a printed DGS is placed outside the area of the coupled loop antenna, instead of the ground plane, as shown in Figure 4(b). The details of this DGS are shown in Figure 4(c). In this case, $w = 2.5\,\text{mm}$, $tx = 1\,\text{mm}$, $ty = 1\,\text{mm}$.

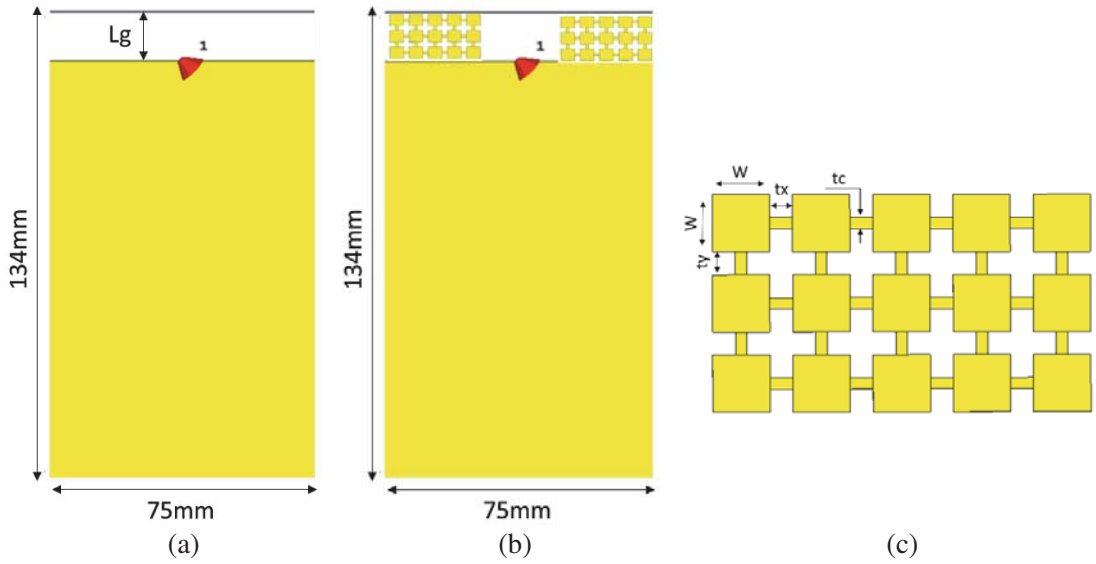

Figure 4. Different configurations of the proposed are antenna based on the ground plane, where Case 1 is a fully grounded plane. (a) Case 2, partially Ground plane. (b) Case 3, partially ground plane loaded by DGS. (c) 5×3 DGS array structure.

The three types of antennas are simulated by using the CST microwave studio suite 2018 simulator. The reflection coefficient is calculated over the required antenna bandwidth from 3 GHz to 5 GHz, and radiation patterns have been calculated over different frequencies. Also, the dimensions of the antenna and the associated DGS have been studied to reach the maximum possible efficiency for the proposed antenna.

2.1. Antenna with Full Ground Plane

Figure 5 shows the reflection coefficient for the antenna with a full ground plane. The resonance of the antenna, in this case, occurs in a small frequency band around 3.45 GHz. However, outside this resonance frequency, the antenna has a quite high reflection coefficient. Figure 6 shows the radiation pattern and the realized gain in dB at the resonant frequency of 3.45 GHz. It can be noted that the antenna has nearly omnidirectional radiation, which is suitable for mobile phone applications. The total antenna efficiency versus frequency of the designed coupled loop antenna with a full ground plane is shown in Figure 7. The maximum total efficiency is 9% at resonant frequency 3.45 GHz.

2.2. Antenna with Partial Ground Plane

The reflection coefficient for the same coupled loop antenna with a partial ground plane is shown in Figure 5. It was also calculated for different values of Lg as shown in Figure 8. It can be noted that the best case occurs where $Lg = 14\,\text{mm}$. In this case, the reflection coefficient is less than $-7\,\text{dB}$ in all the

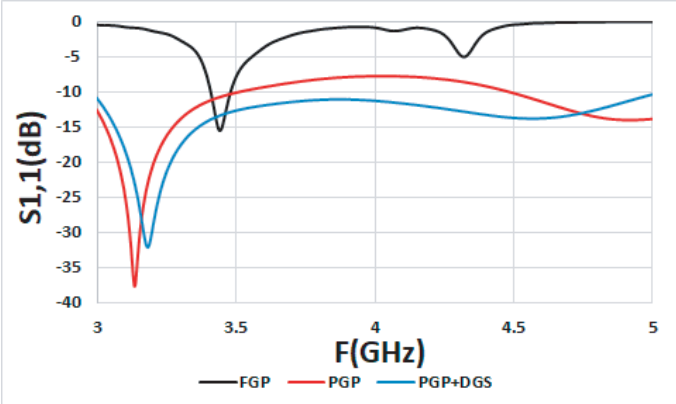

Figure 5. The simulated reflection coefficient of the designed folded dipole antenna for all three configurations.

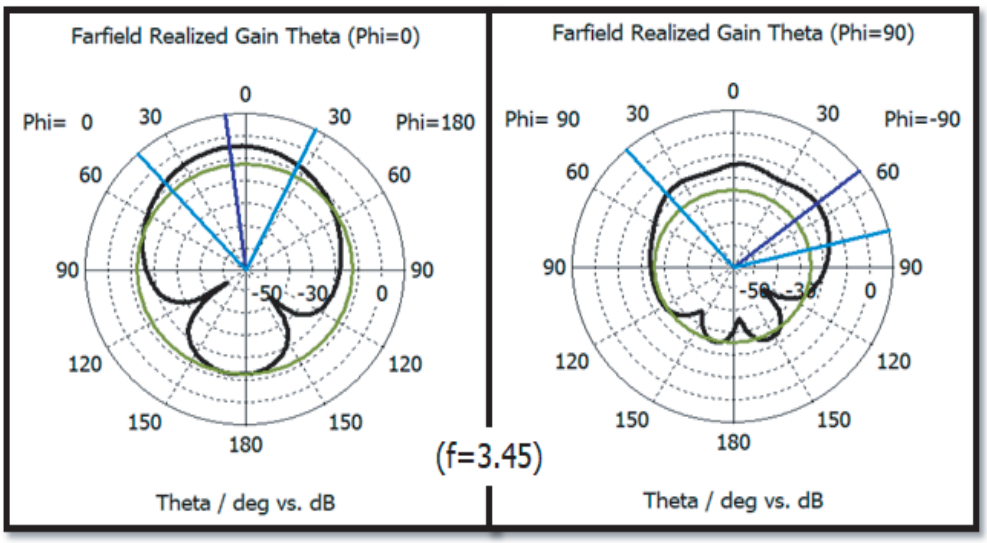

Figure 6. Realized antenna gain of the designed folded dipole antenna with a full ground plane at 3.45 GHz.

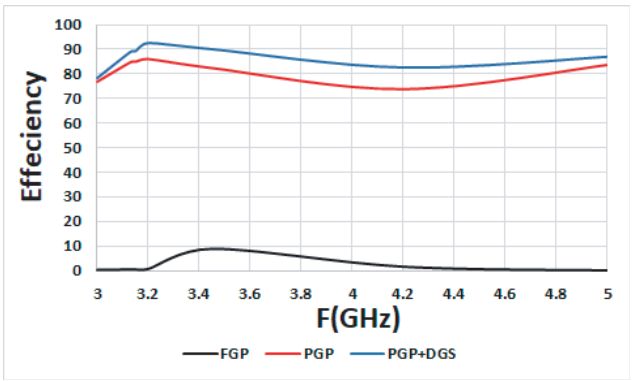

Figure 7. The total efficiency of the designed folded dipole antenna for all three configurations.

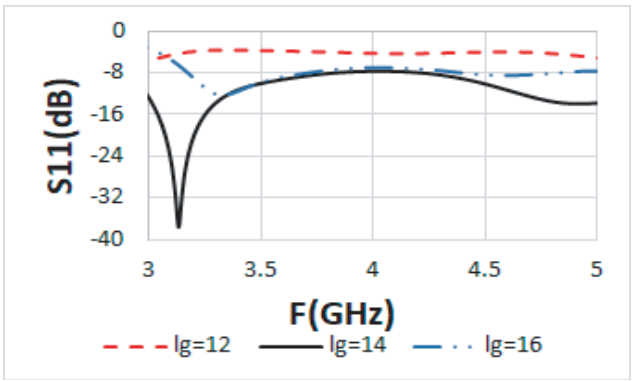

Figure 8. The simulated reflection coefficient of the designed folded dipole antenna with a partial ground plane with variable values of lg.

frequency bands from 3 to 5 GHz. This configuration would be suitable for 5G applications, where the upper limit of the reflection coefficient is −6 dB. The resonance frequency of the antenna in this case is at 3.2 GHz.

The radiation pattern and realized antenna gain at the resonant frequency 3.2 GHz and both ends of the bandwidth of the partial ground plane antenna are shown in Figure 9. It can be noted that the peak antenna gain is around 1.5 dB in this case. The total antenna efficiency versus frequency of the designed coupled loop partial ground plane antenna is shown in Figure 7. The maximum total efficiency at the resonant frequency 3.2 GHz is 86%. The resulting increase in gain and efficiency is due to the improvement in the matching of the antenna compared to the previous case.

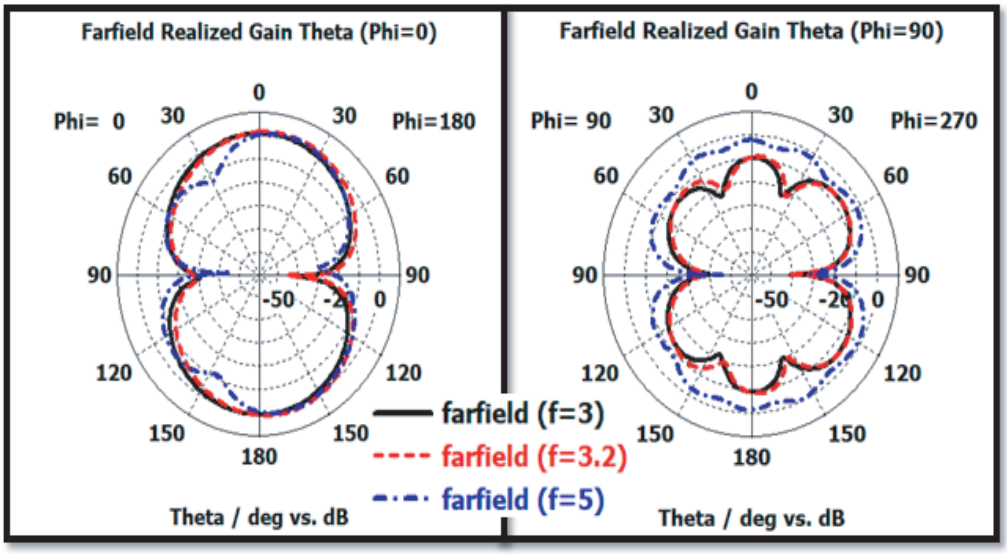

Figure 9. Realized antenna gain of the designed folded dipole antenna with a partial ground plane at different frequencies.

2.3. Partial Ground Antenna with EBG

The third configuration is based on a coupled loop antenna on a partial ground plane loaded by a printed DGS. Figure 5 shows the simulated reflection coefficient of the antenna with the DGS. In this case, the reflection coefficient is less than −10 dB in the antenna bandwidth from 3 to 5 GHz. Using DGS reduces the reflection coefficient of the designed antenna by nearly −2 dB, without reducing the bandwidth. This represents a good modification of the designed antenna. Besides, the resonant frequency is still around 3.2 GHz for this antenna structure.

The radiation pattern and realized antenna gain of the antenna loaded by a DGS are shown in Figure 10. The gain is calculated at both ends of the bandwidth and the resonant frequency 3.2 GHz. It can be noted that the peak antenna gain is around 1.9 dB in this case. Figure 13 shows the total antenna efficiency versus frequency for the designed coupled loop antenna, with a partial ground plane loaded by a DGS. The maximum total efficiency is 92.5% at resonant frequency 3.2 GHz.

3. MIMO ANTENNA STRUCTURE

After reaching acceptable results for the individual antenna by using a printed DGS structure, six antennas of the same type with the same dimensions are combined to form a MIMO antenna. The DGS structures are distributed in arrays 3×5 on the sides of each of the six antennas, in the back surface of the substrate. Figures 11(a) and (b) show the proposed MIMO antenna system with DGS, from the front and back views where $A = 25$ mm, $B = 28$ mm, $C = 40.5$ mm, $D = 40.25$ mm.

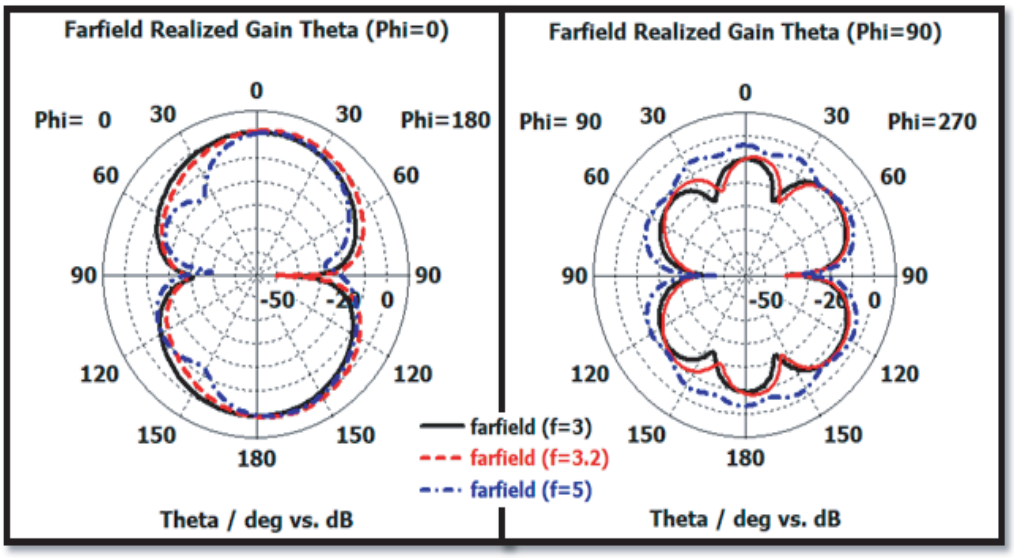

Figure 10. Realized antenna gain of the designed folded dipole antenna with a partial ground plane with DGS at different frequencies.

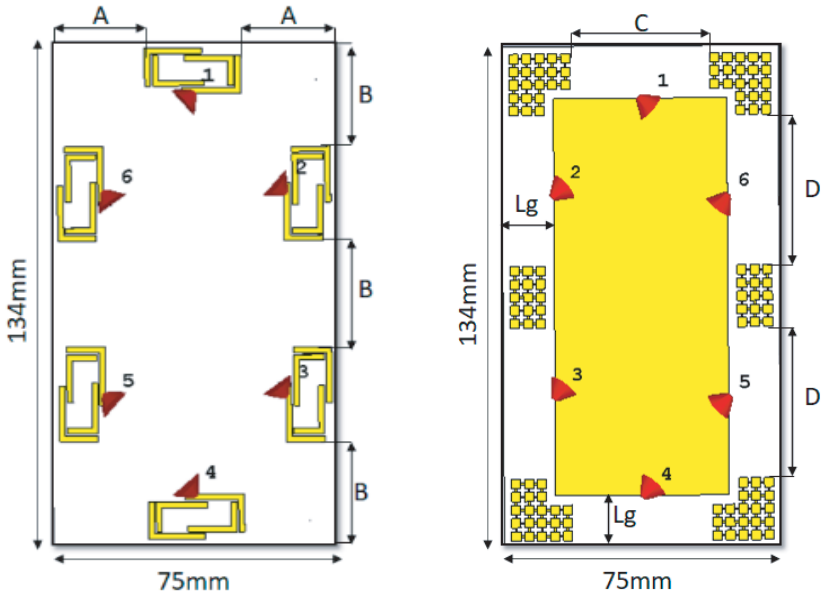

(a) (b)

Figure 11. The Geometry of the proposed 6 element MIMO antenna on a substrate of a size of a mobile phone. (a) Front view. (b) Back view.

Figure 12 shows the reflection coefficient of the six antennas in the MIMO system. The limit of the reflection coefficient factor for the antenna inside the MIMO system is −6 dB. Antennas Nos. 2 and 5 achieved reflection coefficient factor less than −7 dB, while antennas Nos. 1 and 4 achieved reflection coefficient factor less than −8 dB, and antennas Nos. 3 and 6 achieved reflection coefficient factor less than −9 dB.

Figure 13 shows the mutual coupling between the different antenna elements of the MIMO antenna system. Figure 13(a) shows the mutual coupling between antenna No. 1 and the other five antennas. It

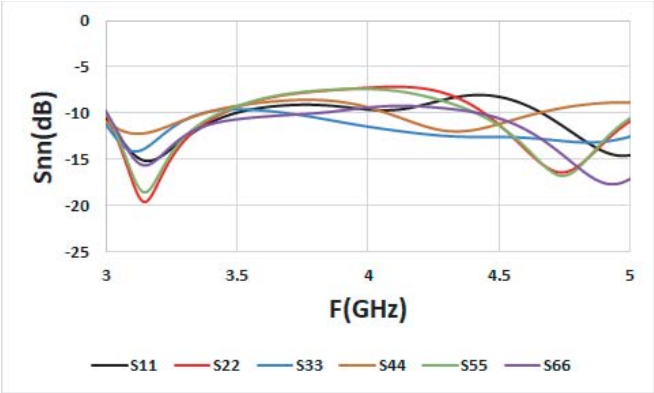

Figure 12. The reflection coefficient of the six antennas constituent MIMO system.

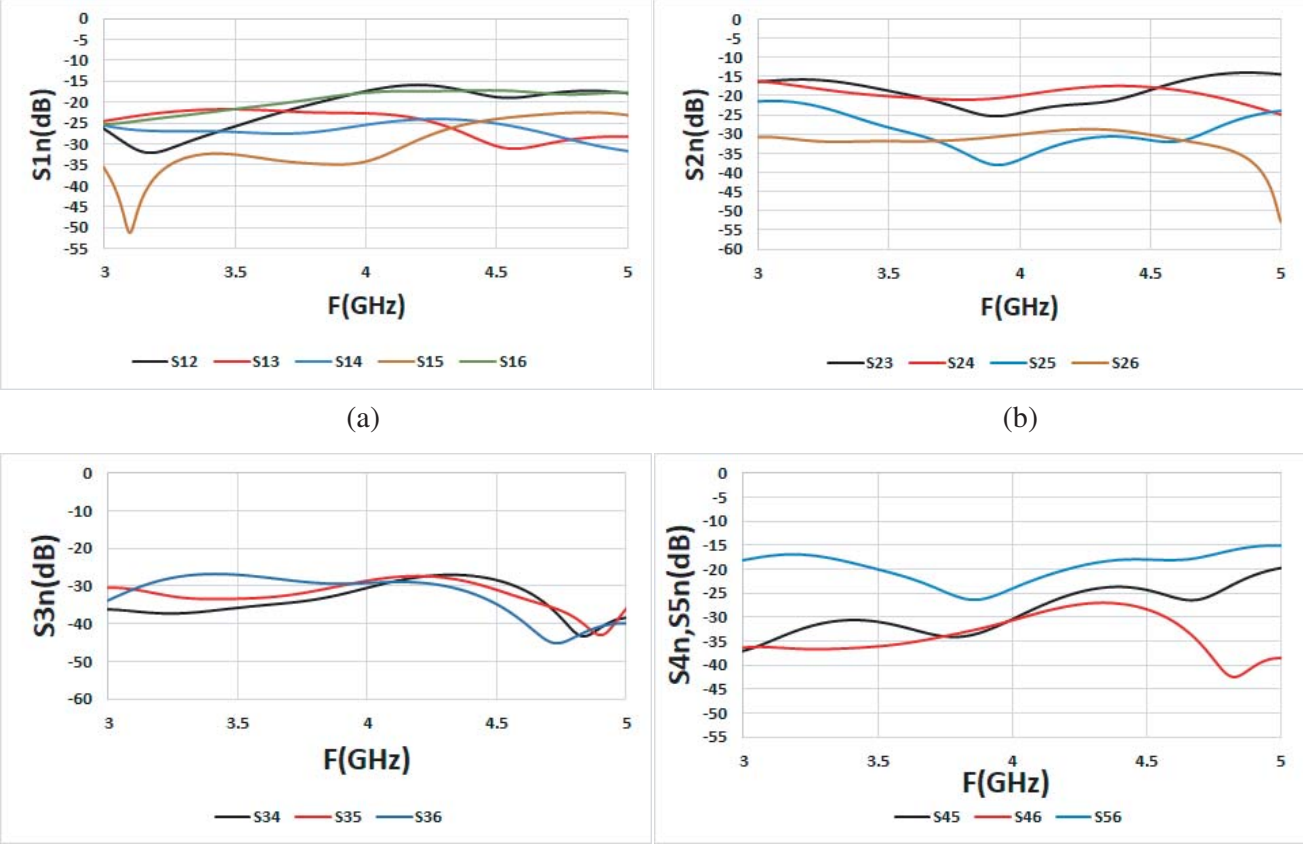

Figure 13. The simulated MIMO system antennas mutual coupling. (a) Antenna 1. (b) Antenna 2. (c) Antenna 3. (d) Antenna 4 and 5.

can be noted that this mutual coupling is less than −20 dB for antennas No. 3, 4, and 5. The mutual coupling is less than −15 dB between antenna No. 1 and the other two antennas; No. 2 and 6. The mutual coupling coefficients between antenna No. 2 and other antennas are shown in Figure 13(b). It can be noted that the mutual coupling is less than −15 dB from antennas No. 3 and 4, −21 dB from antenna No. 5, and −30 dB from antenna No. 6. Figure 13(c) indicates that the mutual coupling between antenna No. 3 and antennas No. 5 and No. 6 is less than −28 dB. Figure 13(d) shows that the mutual

coupling between Antenna No. 4 and antennas No. 5 and 6 is less than −21 dB. In addition, the mutual coupling between antennas No. 5 and 6 is less than −15 dB.

To take into consideration the effect of the hand on the performance of the proposed MIMO antenna, this problem is studied as shown in Figure 14. A comparison between the reflection coefficients for the different antenna elements with and without the hand is presented in Figure 15. It can be noted that the reflection coefficient is slightly increased. However, the reflection coefficient for all elements with the hand is still within the limit of less than −6 dB.

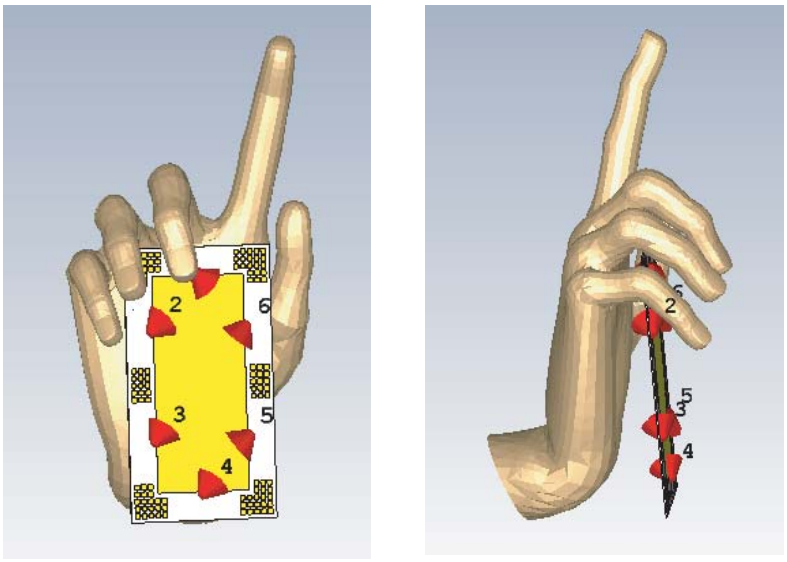

(a) (b)

Figure 14. The MIMO antenna system with hand model. (a) Front view. (b) Side view.

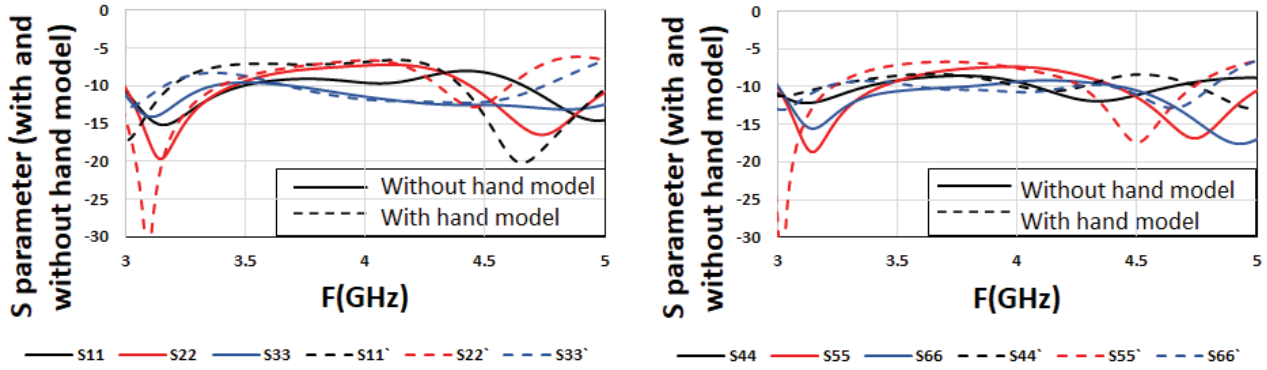

(a) (b)

Figure 15. The difference between the S-parameter in the presence and absence of the hand model.

These S-parameters are used to calculate the corresponding MIMO paper makers of the proposed MIMO antenna configuration.

One of the most important factors affecting the MIMO system is the Envelop Correlation Coefficient (ECC). The ECC between antenna m, and antenna n can be calculated in terms of S-parameter as

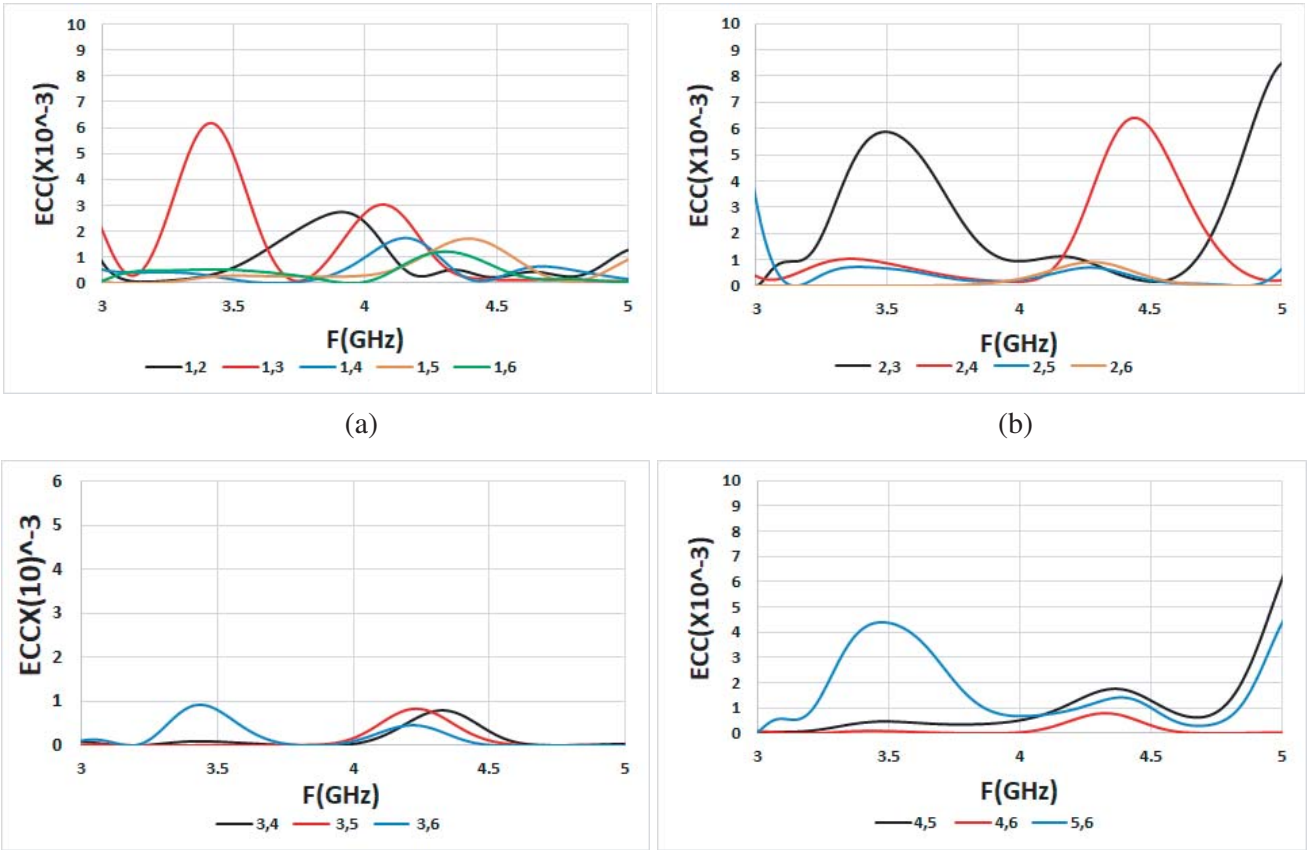

Figure 16. The ECC between MIMO system antennas. (a) $\mathrm{ECC}_{1,n}$. (b) $\mathrm{ECC}_{2,n}$. (c) $\mathrm{ECC}_{3,n}$. (d) $\mathrm{ECC}_{4,n,\ and\ 5,n}$.

follows [16]:

$$ECC_{m,n} = \frac{|S^*_{mm}S_{mn} + S^*_{nm}S_{nn}|^2}{(1 - |S_{mm}|^2 - |S_{mn}|^2)(1 - |S_{nm}|^2 - |S_{nn}|^2)^*} \tag{1}$$

Figure 16 shows the ECC over frequency for the different six antennas of the proposed MIMO antenna system. The value of ECC for all antenna elements is less than 0.006 which lies within the limits of MIMO antenna for 5G application. This result is considered very acceptable for the work of a high-performance MIMO system, as it is required that the ECC parameter be less than 0.5 [17].

Diversity gain (DG) for the MIMO configuration represents the loss in transmission power when diversity schemes are performed on the module. The DG is calculated in terms of ECC as follows [18]:

$$DG = 10\sqrt{1 - |ECC|^2} \tag{2}$$

To ensure a good MIMO antenna system performance in terms of a diversity gain of 10 dB is required for the antenna [18].

Another important parameter to calculate the diversity performance of the MIMO antenna system is the Total Active Reflection Coefficient (TARC) which is given by [16]:

$$\mathrm{TARC}_{m,n} = -\sqrt{\frac{(S_{mm} + S_{mn})^2 + (S_{nm} + S_{nn})^2}{2}} \tag{3}$$

TARC can be defined as the ratio of the square root of reflected power to the incident power. It represents the apparent reflection coefficient of the antenna within the MIMO system. It should be less

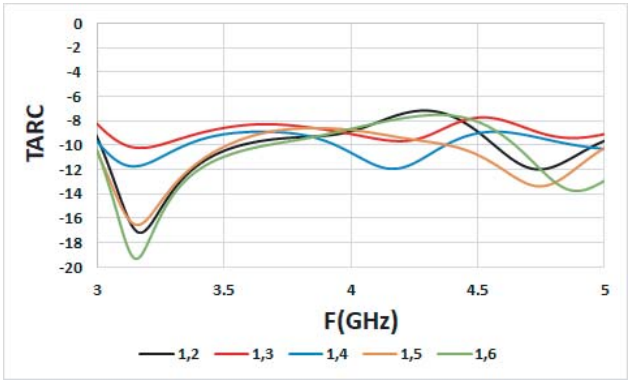

(a)

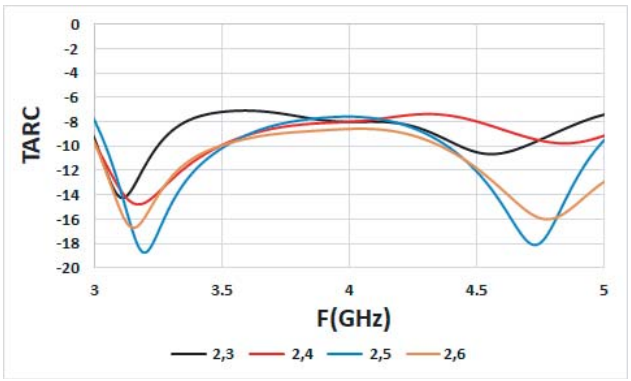

(b)

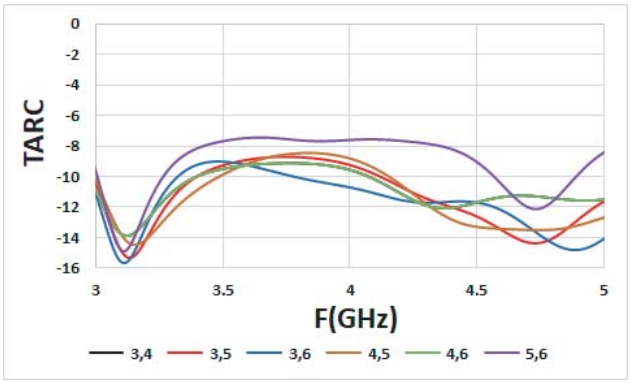

(c)

Figure 17. The TARC between MIMO system antennas. (a) $\mathrm{TARC}_{1,n}$. (b) $\mathrm{TARC}_{2,n}$. (c) $\mathrm{TARC}_{3,n,4,n,\ and\ 5,n}$.

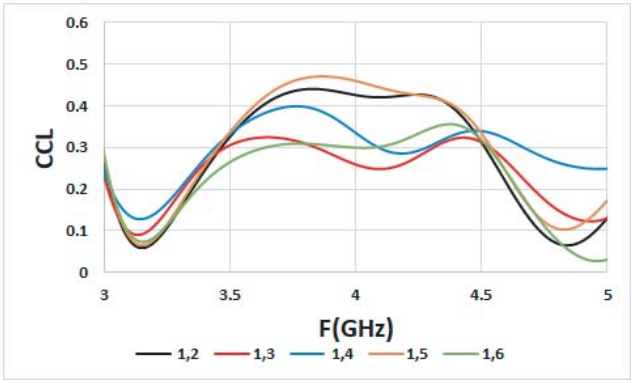

(a)

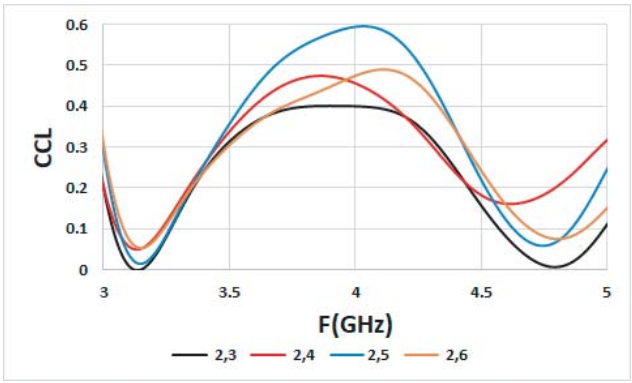

(b)

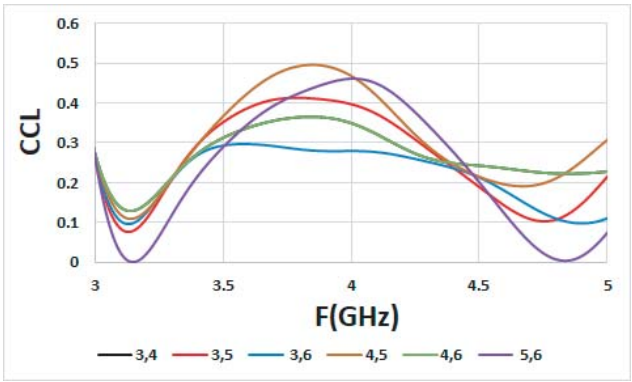

(c)

Figure 18. The CCL between MIMO system antennas. (a) $\mathrm{CCL}_{1,n}$. (b) $\mathrm{CCL}_{2,n}$. (c) $\mathrm{CCL}_{3,n,4,n,\ and\ 5,n}$.

than -6 dB for 5G applications [19]. In this paper, the value of TARC for the proposed antenna is less than -7 dB, as shown in Figure 17.

Channel Capacity Loss (CCL) is among the performance parameters of the MIMO system. CCL information for MIMO systems is calculated according to the correlation effect as follows:

$$\mathrm{ccl}_{i.j} = -\log_2\left(\left|\frac{\sigma_{i,i}}{\sigma_{j,i}}\frac{\sigma_{i,j}}{\sigma_{j,j}}\right|\right) \tag{4}$$

where:

$$\sigma_{i,i} = 1 - \left(|S_{i,i}|^2 - |S_{i,j}|^2\right) \tag{4a}$$

$$\sigma_{i,j} = -\left(S^*_{i,i}S_{i,j} + S_{j,i}S^*_{j,j}\right) \tag{4b}$$

The CCL of the proposed MIMO antenna system is less than the practical standard of 0.6 bit/s/Hz over the bandwidth of the antenna as shown in Figure 18.

Mean Effective Gain (MEG) is the mean received power in the radiation environment. The MEG analysis is an important parameter for determining diversity performance. For acceptable diversity performance, the practical standard of MEG should satisfy the condition that $-3 \leq MEG\,(\text{dB}) < -12$, for all MIMO antennas of the proposed system [8]. The MEG value of our MIMO system is shown in Figure 19, and it can be calculated as follows:

$$\text{MEG}_i = 0.5\mu_{irad} = 0.5\left(1 - \sum\nolimits_{j=1}^{k} |S_{i,j}|\right) \tag{5}$$

where i represents the antenna under observation, μ_{irad} the radiation efficiency, and k the number of antennas. The MEG for the designed MIMO antenna is shown in Figure 19. It can be noted that the obtained MEG lies within the required range where it varies between -3.5 dB and -7.3 dB.

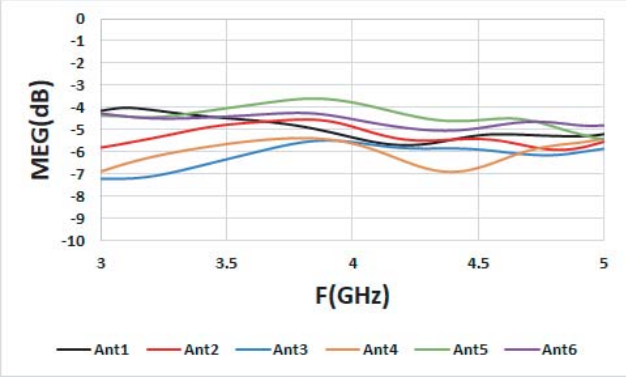

Figure 19. The MEG of MIMO system antennas.

Figure 20. Fabricated folded dipole antenna with a partial ground plane loaded by printed DGS.

4. SAR CALCULATION

In Table 1, the SAR analyses of the three individual antenna configurations are presented. These analyses are calculated at resonant frequency 3.2 GHz and another randomly chosen frequency of 4.2 GHz. The hand and head model, which is included in the CST microwave studio simulator shown in Figure 14, has been used to calculate SAR over 1 g tissue. From this table, it is clear that the best antenna configuration in terms of SAR reduction is the type that uses Full Ground

Table 1. Simulated SAR calculations for the three individual antenna Configurations at different frequencies.

SAR (W/kg)		Frequency (GHz)	
		3.2 GHz	4.2 GHz
Antenna configuration	FGP	0.00089	0.00061
	PGP	0.50642	0.08592
	PGP + DGS (proposed)	0.19256	0.25698

Table 2. Simulated SAR calculations for the MIMO antenna system at different frequencies.

Frequency (GHz)	SAR (W/kg)						
	Antenna						
	Antenna (1)	Antenna (2)	Antenna (3)	Antenna (4)	Antenna (5)	Antenna (6)	Total
3.2 GHz	0.37285	0.12626	0.16959	0.11053	0.31866	0.36089	1.45878
4.2 GHz	0.55737	0.2452	0.42322	0.16989	0.38876	0.21312	1.99756

Plane (FGP). The partial ground plane PGP and PGP loaded by DGS configurations give close values regarding SAR reduction. Although all three configurations give a SAR value less than the permissible international limits, the antenna with DGS provides also a good reflection coefficient, high gain, and broad bandwidth. Therefore, the DGS configuration has been chosen to be the final proposed individual antenna configuration, and it has been used to create a MIMO system. Table 2 presents SAR analysis of the proposed MIMO antenna system also at frequencies 3.2 GHz and 4.2 GHz. The SAR value for each antenna is calculated separately as well as the total SAR value for the MIMO system.

5. EXPERIMENTAL RESULTS

Figure 20 shows the fabricated coupled folded dipole antenna with a PGP loaded by DGS. Figure 21 shows the measurement process of the reflection coefficient, and Figure 22 shows a comparison between the simulated and measured reflection coefficients for the fabricated antenna. It can be noted that the measured reflection coefficient for the fabricated antenna is still less than −10 dB on the entire operating bandwidth. However, the resonance around 3.2 GHz is slightly shifted up to around 3.3 GHz in the experimental. The effect of soldering the connector could be the reason for this slight change in the resonance behavior. However, this slight change does not have a significant effect on the matching and the required operating bandwidth of the fabricated antenna.

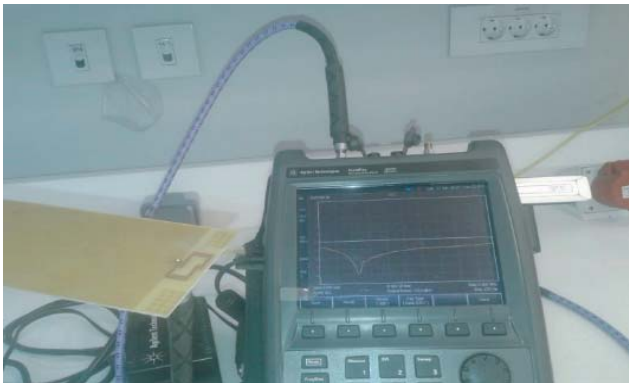

Figure 21. Measurement of the fabricated antenna.

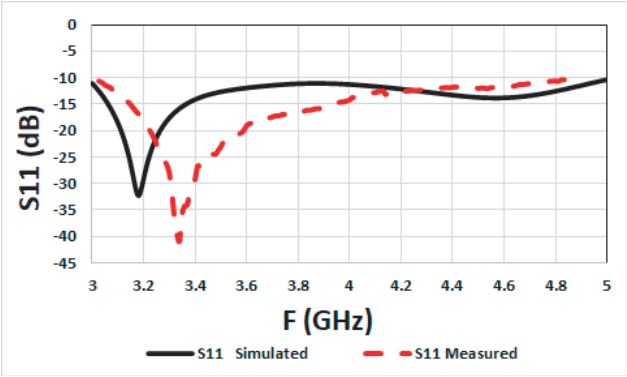

Figure 22. Comparison between simulated and measured reflection coefficient of the designed folded dipole antenna with a partial ground plane loaded by printed DGS.

The proposed MIMO antenna is also fabricated and measured for verification. Figure 23 shows the 6-element fabricated MIMO antenna system with a PGP loaded by DGS. Figure 24 shows the measured reflection coefficients of the fabricated MIMO antenna elements. On the other hand, Figure 25, shows the coupling coefficients between the different elements. It can be noted that the measured results are very close to the simulated results presented in the previous sections.

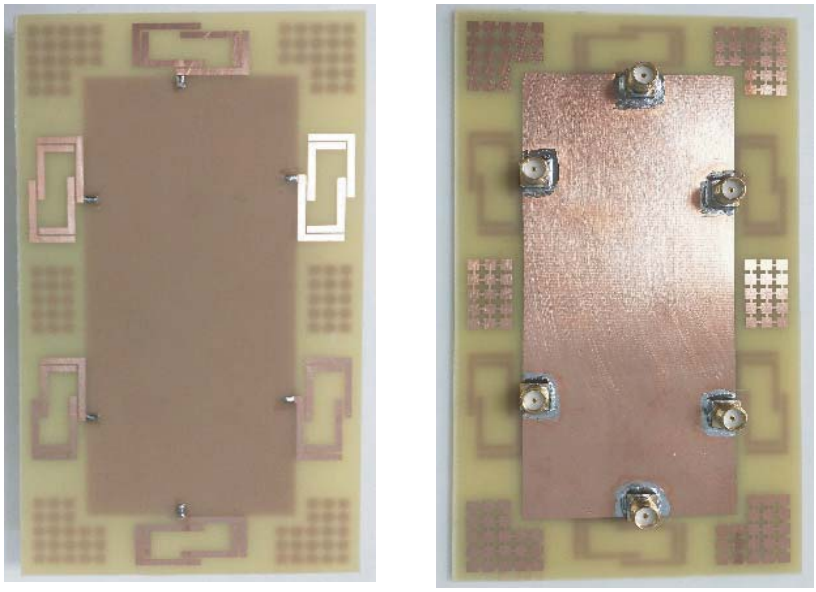

(a) (b)

Figure 23. The fabricated MIMO antenna. (a) Front view. (b) Back view.

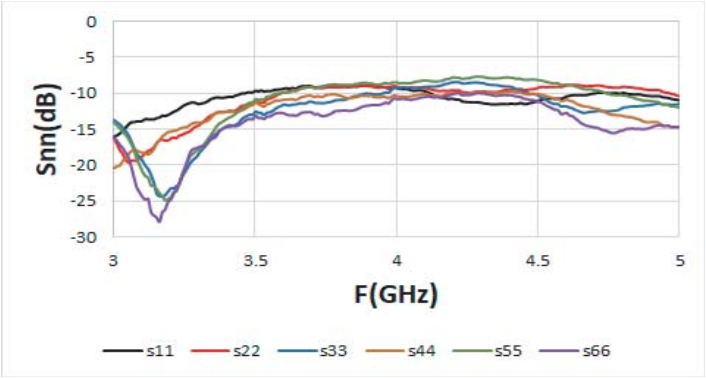

Figure 24. The Reflection coefficient for the six antennas of the fabricated MIMO antenna system.

Table 3. Comparison between the proposed antenna and the most recent similar works in terms of MIMO parameters.

Reference	ECC	$DG = (10\,\text{dB})$	TARC	CCL (bit/sec/Hz)	MEG (dB)
[17]	< 0.05	Not valid	Not valid	Not valid	Not valid
[18]	< 0.01	$\surd$	Not valid	< 0.4	$-3 < MEG < -9$
[19]	< 0.21	Not valid	Not valid	< 0.32	Not valid
[20]	< 0.016	$\surd$	$< -35\,\text{dB}$	< 0.3	$< -3\,\text{dB}$
[21]	< 0.05	Not valid	Not valid	Not valid	Not valid
[22]	< 0.015	$\surd$	$f < -10\,\text{dB}$	Not valid	Not valid
This work	< 0.006	$\surd$	$< -7\,\text{dB}$	< 0.6	$-3 < MEG < -8$

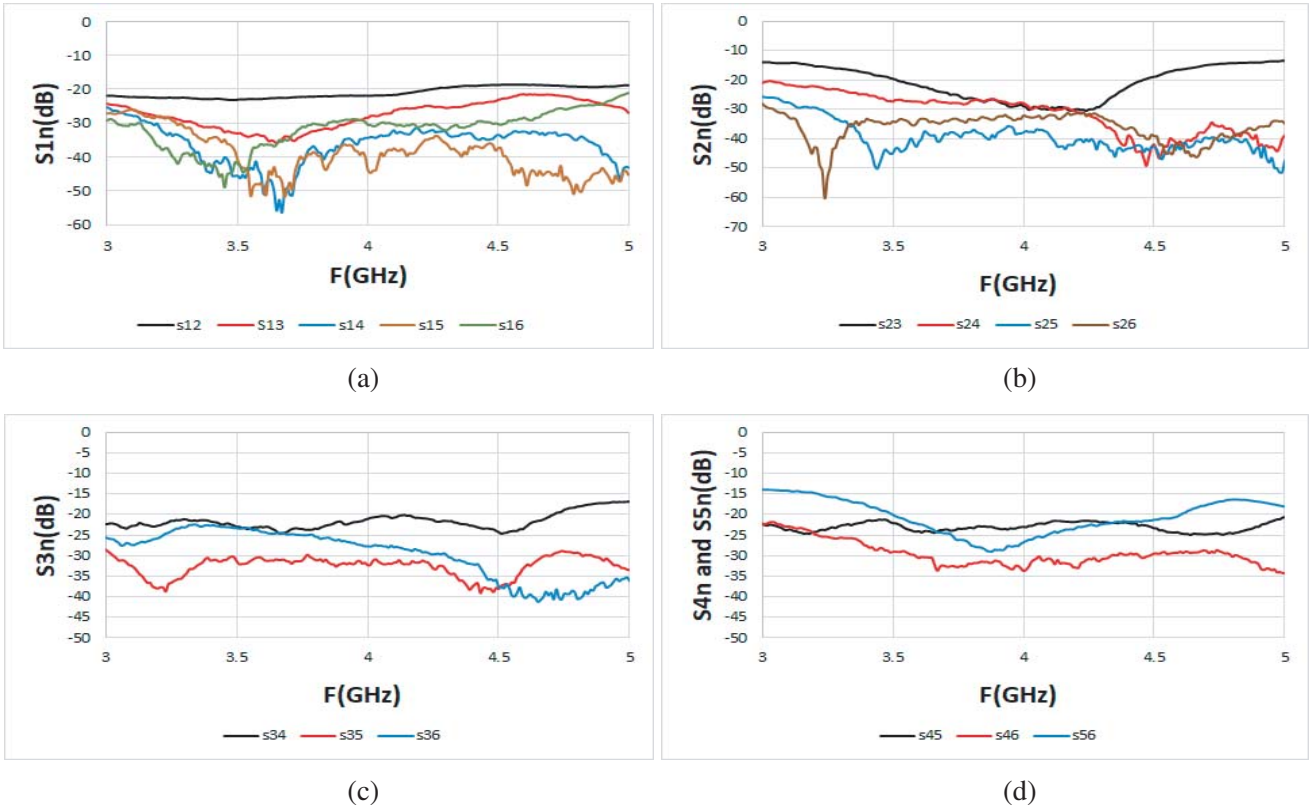

Figure 25. The simulated MIMO system antennas mutual coupling. (a) Antenna 1. (b) Antenna 2. (c) Antenna 3. (d) Antenna 4 and 5.

Table 4. Comparison between the proposed antenna and the most recent similar works in terms of the most important characteristics required for the antenna.

Reference	Antenna type	Bandwidth	Return Loss (over the bandwidth)	No-of elements	Isolation method	Isolation	Antenna size	Peak SAR value	Application
[17]	3-D folding technique	Multi bands	< -6 dB	2	FSS patches	< -30 dB	$(50 \times 70 \times 1.6)$ mm^3	Not valid	WLAN, Wi-MAX, 5G cellular, and 5G Wi-Fi
[18]	Rectangular shape-slotted patch antenna	(25.5–29.6) GHz	< -10 dB	4	DGS	< -10 dB	$(30 \times 35 \times 0.76)$ mm^3	Not valid	mm-waveband for 5G applications
[19]	Monopole antenna	(2.4–2.7) GHz and (3.3–3.6) GHz	< -6 dB	8	Grounding branch	< -15 dB	$(124 \times 74 \times 4)$ mm^3	< 1 W/kg	5G smartphone application
[20]	Circular patch with shapes extruded	(8–12) GHz	< -10 dB	2	EBG structure	< -22 dB	$(55 \times 49 \times 1.6)$ mm^3	Not valid	X-band, radar, and sbx-1 applications
[21]	Coupled loop antenna	(3.3–5) GHz	< -10 dB	8	Not valid	< -15 dB	$(75 \times 134 \times 6.8)$ mm^3	Not valid	N77, N78, and N79 applications
[22]	Novel design	(3.3–4.4) GHz, (5–6) GHz, and (7.9–8.6) GHz	Not valid	2	TVC-EBG structure	< -15 dB	$(21 \times 36 \times 1.6)$ mm^3	Not valid	UWB-MIMO wireless communication
This work	Coupled folded antenna	(3–5) GHz	< -7 dB	6	DGS	< -15 dB	$(134 \times 75 \times 0.8)$ mm^3	< 2 W/kg	N77, N78, and N79, 5G applications

Finally, a detailed comparison between the proposed antenna and previously published related antenna configurations in terms of MIMO parameters is presented in Table 3. Another comparison in terms of the important parameters is presented in Table 4. In Table 3, it is clear that the proposed MIMO system achieves promising MIMO parameter values. From Table 4 it is clear that the present design is distinguished by its wide bandwidth which includes all bands of sub-six 5G communications. It is also distinguished from References [17] and [19] in terms of reflection coefficient. Low mutual coupling values and compatible size which are suitable for mobile communications are also achieved by the proposed MIMO antenna.

6. CONCLUSION

A new design of folded dipole antennas with multi-coupled sections is presented as an antenna element in a MIMO antenna with six radiators. This MIMO antenna is suitable for the N77, N78, and N79 bands of 5G Communication systems. The configuration of the individual antenna design consists of a folded dipole antenna with four coupled sections placed at the edges of the smartphone board with a partial ground plane less than the antenna element. A DGS is added between the antenna elements to improve the return loss factor and to reduce the coupling between the antenna elements in the MIMO system. The MIMO system provides good return loss, low mutual coupling, and a wideband of frequency. Fundamental parameters of the presented MIMO design are investigated, and very good results are obtained. Prototype samples of the proposed individual antenna and the proposed MIMO system were fabricated and measured. The fabricated antennas show good agreement with the simulated results.

REFERENCES

1. Sun, L., Y. Li, Z. Zhang, and Z. Feng, "Wideband 5G MIMO antenna with integrated orthogonal-mode dual-antenna pairs for metal-rimmed smartphones," *IEEE Transactions on Antennas and Propagation*, Vol. 68, No. 4, 2494–2503, 2019.
2. Liu, H. Y. and C. J. Huang, "Wideband MIMO antenna array design for future mobile devices operating in the 5G NR frequency bands n77/n78/n79 and LTE band 46," *IEEE Antennas and Wireless Propagation Letters*, Vol. 19, No. 1, 74–78, 2019.
3. Tu, D. T. T., N. T. B. Phuong, P. D. Son, and V. Van Yem, "Improving characteristics of 28/38 GHz MIMO antenna for 5G applications by using double-side EBG structure," *Journal of Communications*, Vol. 14, No. 1, 1–8, 2019.
4. Garg, P. and P. Jain, "Isolation improvement of MIMO antenna using a novel flower-shaped metamaterial absorber at 5.5 GHz WiMAX band," *IEEE Transactions on Circuits and Systems II: Express Briefs*, Vol. 67, No. 4, 675–679, 2019.
5. Khade, S. S. and S. L. Badjate, "Square shape MIMO antenna with defected ground structure," *4th International Conference on Recent Advances in Information Technology (RAIT)*, 1–5, 2018.
6. Hu, W., X. Liu, S. Gao, L. Wen, Q. Luo, P. Fei, Y. Yin, and Y. Liu, "Compact wideband folded dipole antenna with multi-resonant modes," *IEEE Transactions on Antennas and Propagation*, Vol. 67, No. 11, 6789–6799, Nov. 2019.
7. Banerjee, J., A. Karmakar, R. Ghatak, and D. R. Poddar, "Compact CPW-fed UWB MIMO antenna with a novel modified Minkowski fractal Defected Ground Structure (DGS) for high isolation and triple band-notch characteristic," *Journal of Electromagnetic Waves and Applications*, Vol. 31, No. 15, 1550–1565, 2017.
8. Rao, T. V., A. Sudhakar, and K. P. Raju, "Novel technique of MIMO antenna design for UWB applications using defective ground structures," *Journal of Scientific & Industrial Applications*, Vol. 77, No. 1, 66–69, 2018.
9. Hota, S., S. Baudha, B. B. Mangaraj, and M. V. Yadav, "A compact, ultrawideband planar antenna with modified circular patch and a defective ground plane for multiple applications," *Microwave and Optical Technology Letters*, Vol. 61, No. 9, 2088–2097, 2019.

10. Sheeba, I. R., B. Velan, and M. Sugadev, "Design and analysis of energy band gap and defective ground structure on array of patch antenna using meta material," *2020 Third International Conference on Smart Systems and Inventive Technology (ICSSIT)*, IEEE, 2020.
11. Bhattacharjee, S., M. Mitra, and S. R. Bhadra Chaudhuri, "An effective SAR reduction technique of a compact meander line antenna for wearable applications," *Progress In Electromagnetics Research* Vol. 55, 143–152, 2017.
12. Hota, S., S. Baudha, B. B. Mangaraj, and M. V. Yadav, "A compact, ultrawideband planar antenna with modified circular patch and a defective ground plane for multiple applications," *Microwave and Optical Technology Letters*, Vol. 61, No. 9, 2088–2097, 2019.
13. Parchin, N. O., H. J. Basherlou, Y. I. Al-Yasir, A. M. Abdulkhaleq, R. A. Abd-Alhameed, and P. S. Excell, "Eight-port MIMO antenna system for 2.6 GHz LTE cellular communications," *Progress In Electromagnetics Research*, Vol. 99, 49–59, 2020.
14. Saleem, R., M. Bilal, H. T. Chattha, S. U. Rehman, A. Mushtaq, and M. F. Shafique, "An FSS based multiband MIMO system incorporating 3D antennas for WLAN/WiMAX/5G cellular and 5G Wi-Fi applications," *IEEE Access*, Vol. 7, 144732–144740, 2019.
15. Molins-Benlliure, J., M. Cabedo-Fabrés, E. Antonino-Daviu, and M. Ferrando-Bataller, "Effect of the ground plane in UHF chip antenna efficiency," *2020 14th European Conference on Antennas and Propagation (EuCAP)*, 1–5, IEEE, Mar. 2020.
16. Parchin, N. O., H. J. Basherlou, Y. I. Al-Yasir, A. M. Abdulkhaleq, R. A. Abd-Alhameed, and P. S. Excell, "Eight-port MIMO antenna system for 2.6 GHz LTE cellular communications," *Progress In Electromagnetics Research*, Vol. 99, 49–59, 2020.
17. Saleem, R., M. Bilal, H. T. Chattha, S. U. Rehman, A. Mushtaq, and M. F. Shafique, "An FSS based multiband MIMO system incorporating 3D antennas for WLAN/WiMAX/5G cellular and 5G Wi-Fi applications," *IEEE Access*, Vol. 7, 144732–144740, 2019.
18. Khalid, M., S. I. Naqvi, N. Hussain, M. Rahman, S. S. Mirjavadi, M. J. Khan, and Y. Amin, "4-port MIMO antenna with defected ground structure for 5G millimeter-wave applications," *Electronics*, Vol. 9, No. 1, 71, 2020.
19. Jiang, W., Y. Cui, B. Liu, W. Hu, and Y. Xi, "A dual-band MIMO antenna with enhanced isolation for 5G smartphone applications," *IEEE Access*, Vol. 7, 112554–112563, 2019.
20. Saxena, G., P. Jain, and Y. K. Awasthi, "High isolation EBG based MIMO antenna for X-band applications," *2019 6th International Conference on Signal Processing and Integrated Networks (SPIN)*, IEEE, 2019.
21. Zhao, A. and Z. Ren, "Wideband MIMO antenna systems based on coupled-loop antenna for 5G N77/N78/N79 applications in mobile terminals," *IEEE Access*, Vol. 7, 93761–93771, 2019.
22. Thakur, E., N. Jaglan, and S. D. Gupta, "Design of compact triple band-notched UWB MIMO antenna with TVC-EBG structure," *Journal of Electromagnetic Waves and Applications*, Vol. 34, No. 11, 1601–1615, 2020.